Engineering geophysical investigation of permafrost conditions underneath airfield embankments in Northern Quebec (Canada)

Richard Fortier & Catherine Savard
Centre d'études Nordiques (CEN), Université Laval, Québec, QC, Canada
Département de géologie et de génie géologique, Université Laval, Québec, QC, Canada

ABSTRACT
An increase in air temperature in excess of 3 °C over a 10-year period from 1992 to 2002 was observed in Northern Quebec (Canada). This increase induced widespread permafrost degradation in the discontinuous permafrost zone mainly under the form of localized zones of thaw subsidence affecting the performance of roads and airfields built on thaw-instable frozen ground. In a context of fast population growth and increasing resource development in Northern Quebec, the vulnerability of transportation infrastructure to permafrost degradation raises concern for the safety and economic sustainability of the Inuit communities. An engineering geophysical investigation, including capacitively coupled resistivity (CCR) and ground penetrating radar (GPR) surveys, was carried out in summer 2004 at the airports of Tasiujak, Aupaluk, Kangirsuk, and Quaqtaq in Ungava Bay to characterize the frozen ground conditions underneath the airfield embankments and assess their vulnerability to permafrost degradation. CCR and GPR are complementary non-invasive subsurface investigation tools. CCR is effective for characterizing the permafrost conditions while GPR defines accurately the cryostratigraphic contacts. The combined interpretation of CCR and GPR surveys leads to a high resolution cross–section of permafrost conditions. An example of the subsurface characterization capabilities of combined CCR and GPR surveys is given for Tasiujaq Airport which is considered vulnerable to permafrost degradation.

RÉSUMÉ
Une augmentation de la température de l'air supérieure à 3 °C a été observée au Québec nordique (Canada) sur une période de 10 ans de 1992 à 2002. Cette augmentation a provoqué une dégradation généralisée du pergélisol dans la zone de pergélisol discontinu sous la forme de secteurs bien définis d'affaissement au dégel qui affecte la performance des routes et pistes d'atterrissage construites sur un sol gelé instable au dégel. Dans un contexte de forte croissance de la population et de développement de l'exploitation des ressources naturelles au Québec nordique, la vulnérabilité des infrastructures de transport à la dégradation du pergélisol soulève des inquiétudes sur la sécurité et le développement durable des communautés Inuites. Un programme d'investigation géophysique qui incluait des profilages de résistivité électrique avec un système couplé capacitivement et des levés de géoradar a été réalisé durant l'été 2004 aux aéroports de Tasiujaq, Aupaluk, Kangirsuk et Quaqtaq sur la côte ouest de la Baie d'Ungava pour caractériser les conditions de la sous-fondation pergélisolée des remblais aéroportuaires et évaluer leur vulnérabilité à la dégradation du pergélisol. Le système couplé capacitivement et le géoradar sont des outils géophysiques complémentaires d'investigation non-invasive de la sous-surface. Le premier outil fournit des informations sur les conditions du pergélisol alors que le second définit précisément les contacts cryostratigraphiques. L'interprétation combinée des levés de résistivité électrique et de géoradar génère des vues en coupe à haute résolution des conditions du pergélisol. Un exemple des possibilités de caractérisation de la sous-surface avec des levés combinés de résistivité électrique et de géoradar est donné pour l'aéroport de Tasiujaq jugé vulnérable à la dégradation du pergélisol.

1 INTRODUCTION

There are fourteen Inuit communities located along the coasts of Hudson Bay and Ungava Bay in Northern Quebec (Canada) for an easy access to the sea since the Inuit are sustained in part by sea food. They have modern facilities such as roads, airfields, seaports, schools, dispensaries, and houses to accommodate the population. These communities are also situated in the marine transgression of Tyrrell and D'Iberville seas following the retreat of the Wisconsin Ice Sheet where frost-susceptible glaciomarine sediments were deposited. Due to the isostatic rebound, once the sediments were exposed to the cold atmosphere, permafrost aggraded. Most infrastructures such as the airports critical to maintain year-round access to these communities are then potentially built on ice-rich frozen ground and vulnerable to permafrost degradation. In a context of fast population growth, increasing resource development and climate warming anticipated over the next decades, the vulnerability of transportation infrastructure to permafrost degradation raises concern for the safety and economic sustainability of the communities in Northern Quebec. An engineering geophysical investigation was carried out in summer 2004 at the airports of Tasiujak, Aupaluk, Kangirsuk, and Quaqtaq in Ungava Bay (Figure 1) to characterize the frozen ground conditions underneath the airfield embankments and assess their vulnerability to permafrost degradation. The results of this investigation for the Tasiujaq Airport are presented herein.

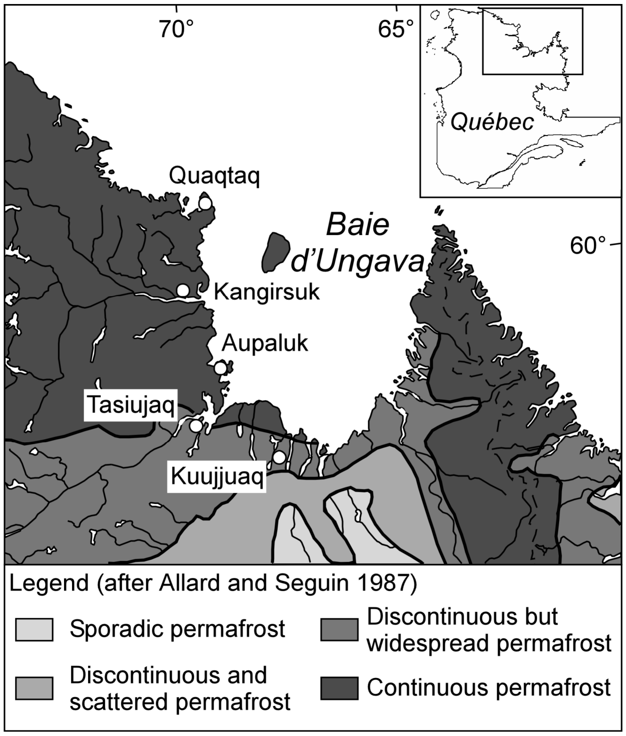

Figure 1. Permafrost distribution and location of Kuujjuaq, Tasiujaq, Aupaluk, Kangirsuk and Quaqtaq in Northern Quebec, Canada.

2 STUDY SITE

The Tasiujaq Airport is located on the West coast of Ungava Bay in the discontinuous but widespread permafrost zone (Figure 1). The airfield is built on a vast marine terrace at an elevation between 29 and 35 m above sea level. According to a stratigraphic cut SC-1 along the Bérard River (Figure 2 and Table 1), the airfield embankment lies on a 2.3 m thick intertidal diamicton near the ground surface made of ice-poor and saline silts and fine sands overlying 7.9 m thick coarse sand and gravel layers over a deep marine clay layer. As observed in the stratigraphic cut SC-1, the intertidal diamicton contains millimetric thick ice lenses. A permafrost mound with a mineral core was levelled at the Northeast end of the airfield from 5+050 and 5+105 m in distance before the embankment construction. The airfield also crosses a small lake which is an abandoned Holocene meander of the Bérard River (Figure 2).

The surface of the airfield embankment is affected by two localized zones of thaw subsidence progressing from the Southeast shoulder to the airfield centre. The subsidence volume of one of these zones was 44 m^3 on July 2004 (Figures 3 and 4). The aircraft pilots complain about this depression in the airfield making hazardous the conditions for take-off and landing. Cracks due to shoulder rotation also affect the embankment sides (Figure 3). The thaw settlement underneath the embankment is taking place in the thaw-instable intertidal diamicton. An increase in air temperature in excess of 3 °C over a 10-year period from 1992 to 2002 was

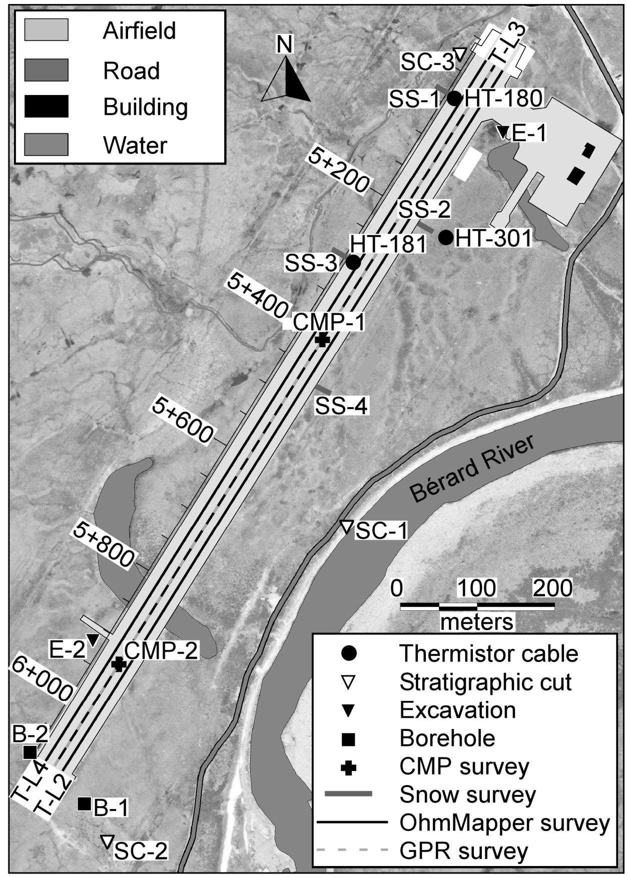

Figure 2. Map of Tasiujaq Airport, Northern Quebec, Canada. Location of geophysical surveys.

Table 1. Description of the stratigraphic cut SC-1 along the Bérard River.

Unit	Characteristics	Depth interval (m)
Organic layer		0 - 0.05 to 0.3
Fluviatile layer	coarse sands	0.05 to 0.3 - 0.7
Intertidal diamicton layer	frost-susceptible and thaw instable silts and fine to coarse sands water content: 2 - 20% pore water salinity: 5 - 18 g/l	0.7 - 3
Coarse sand layer	ice-poor coarse sands, gravels, pebbles and blocks	3 - 4 m
Gravel layer	ice-poor gravels water content: 10 - 15%	4 - 10.9
Deep clay layer	marine clay	> 10.9

observed at Kuujjuaq, about 110 km Southeast of Tasiujaq (Figures 1 and 5). Following this increase in air temperature, permafrost warming was also monitored at Tasiujaq Airport (Figure 6): 1) 3.1 °C at a depth of 7 m in the field from 1994 to 2004 and 2) 1.8 and 0.8 °C at a depth of 5.4 m in the subgrade underneath the airfield embankment and distances of 5+090 m from 1994 to 2004 and 5+300 m from 1992 to 2004 respectively. The depth of the thawing front on July increased by less than 20 cm over the ten-year monitoring period (Figure 6). Moreover, due to Southwest prevailing winds in winter, there is important snow accumulation on the Southeast shoulder and toe of the airfield embankment (Figures 7 and 8) while the tundra away of the airfield is nearly free of snow following the wind ablation. The thick embankment disrupts the topography and acts as a snow fence. The permafrost degradation is therefore due to not only the increase in air temperature but also the thermal insulation of snow cover. This is not unique to the Tasiujaq Airport (Fortier and Bolduc 2008). Drainage problem observed along the embankment toes (Figure 7) can also cause the permafrost degradation due to the latent heat of water delaying the freeze up and cooling of the active layer in winter.

Figure 3. Thaw subsidence and cracks affecting the airfield embankment near the distance 5+230 m, Southeast side, on summer 2001 at Tasiujaq Airport, Northern Quebec, Canada. The black camera case gives the scale. (photograph by Denis Sarrazin, CEN)

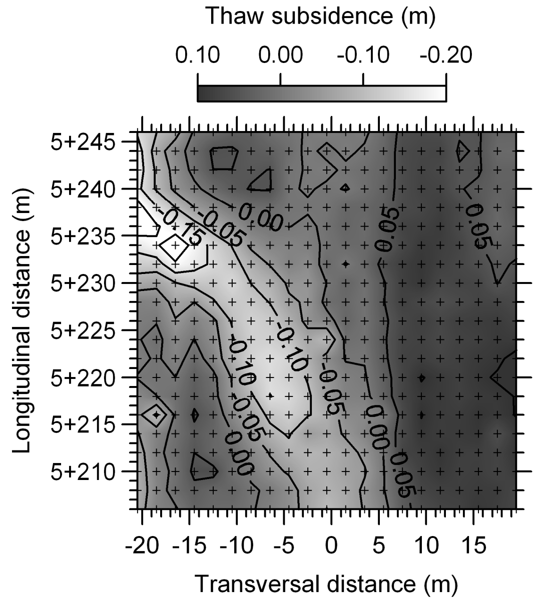

Figure 4. Spatial distribution of thaw subsidence affecting the airfield embankment near the distance 5+230 m, Southeast side, on July 2004 at Tasiujaq Airport, Northern Quebec, Canada. The + symbols identify the location of elevation measurements.

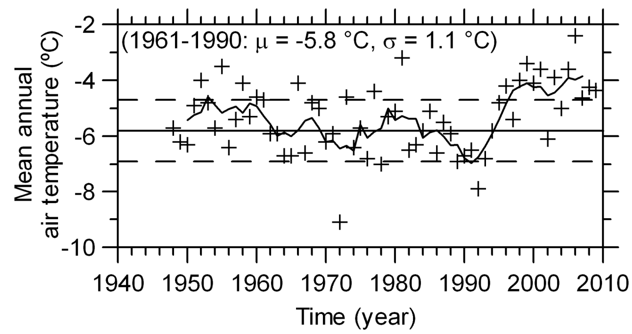

Figure 5. Mean annual air temperature at Kuujjuaq (meteorological record from Environment Canada, http://climate.weatheroffice.gc.ca/index.html). The full curve is a 5 year running average while the full and dashed horizontal lines are respectively the average and ±standard deviation (values in parentheses) over the reference period 1961–1990.

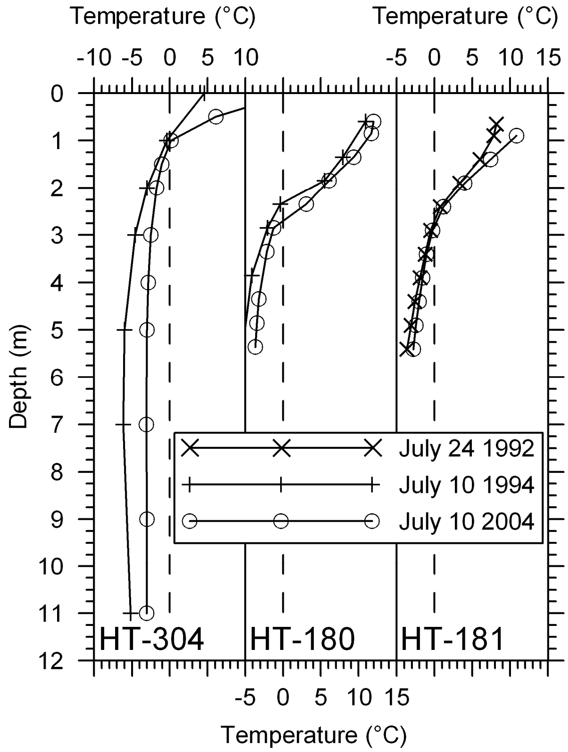

Figure 6. Temperature profiles in the field (HT-304) and in the airfield embankment and subgrade (HT-180 and HT-181) at Tasiujaq Airport, Northern Quebec, Canada. See Figure 3 for the location of thermistor cables HT-304,
HT-180 and HT-181.

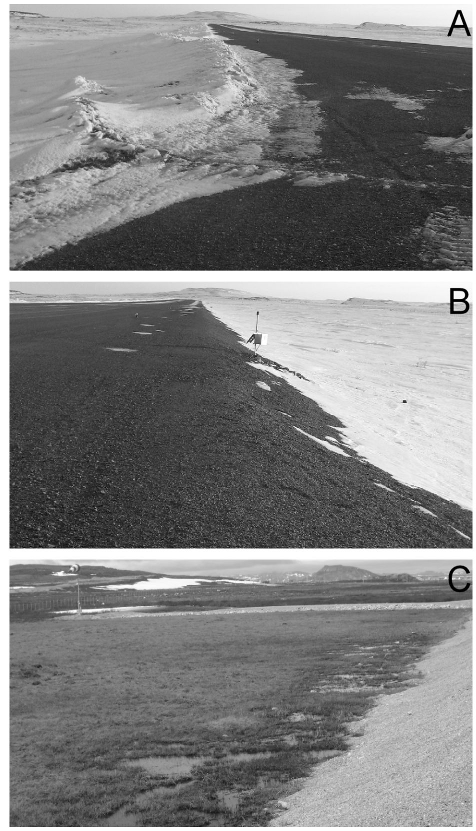

Figure 7. Snow accumulation on the Southeast (A) and Northwest (B) shoulders and toes of the airfield embankment on April 2005. C) Drainage problem at the Northwest toe of the airfield embankment on July 2004 at Tasiujaq Airport, Northern Quebec, Canada. (photographs by Frédéric Vinet, CEN)

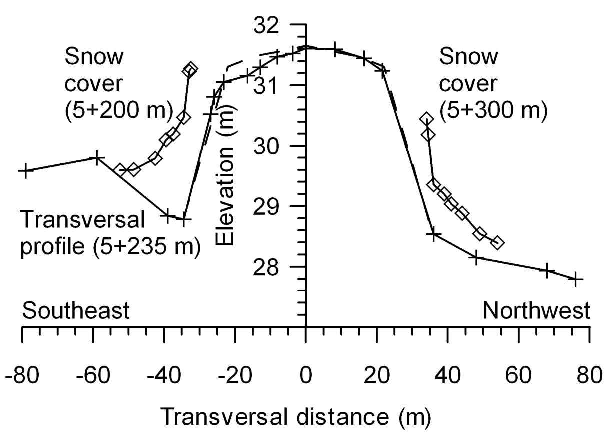

Figure 8. Elevation of the embankment surface on July 2004 and snow surface on April 2005 on the Southeast and Northwest shoulders and toes of the airfield embankment at Tasiujaq Airport, Northern Quebec, Canada. The dash line is the transversal profile as built (MTQ 1990). Note the vertical exaggeration 1:40.

3 ENGINEERING GEOPHYSICAL INVESTIGATION

Capacitively coupled resistivity (CCR) and ground penetrating radar (GPR) surveys were carried out in summer 2004 at the Airport of Tasiujak to assess the spatial variability of frozen ground conditions underneath the airfield embankment. These geophysical tools used along the same survey line are complementary methods (De Pascale et al. 2008). While CCR is effective for characterizing the state of the permafrost, it does not define well the subsurface stratigraphic contacts. GPR, on the other hand, defines accurately the stratigraphy contacts, but does not provide as much information with respect to the state of the permafrost. The combined interpretation of the CCR and GPR can therefore lead to a high resolution cross-section of permafrost conditions. They were successively used to map massive ice, ice wedges, thermokarst, and basic stratigraphic relationships (De Pascale et al. 2008). CCR was also used alone to map frozen glaciofluvial sediments (Calvert 2002) and mountain permafrost in the Swiss Alps (Hauck and Kneisel 2006). There are also CCR applications in unfrozen environments (Douma et al. 1994).

3.1 Capacitively coupled resistivity (CCR) surveys

The Capacitively Coupled Resistivity (CCR) system is made of one transmitter and from one to five receivers to achieve a dipole-dipole configuration. The transmitter and receivers are coaxial cables lying on the ground as antennas to couple an AC signal into the ground and measure the induced AC signal respectively. The conductor in the coaxial cable acts as one plate of a capacitor and the ground acts as the other plate while the insulating sheath of the coaxial cable is the capacitor's insulator. The AC current in the transmitter cable can pass into the ground similarly to an AC signal through a capacitor. The capacitance of the receiver cable is similarly charged, allowing the measurement of an induced AC voltage in the receiver proportional to the electrical resistivity of the ground. This provides an AC equivalent of a standard DC resistivity measurement without the galvanic contacts needed for the standard method (for more details on the theory behind CCR, see Timofeev et al. 1994 and Kuras et al 2006). This is a major advantage since it can be hard to drive electrodes in engineered structures such as a pad of highly compacted crushed rocks of an embankment. Moreover, since the system does not depend on surface contact, it can be towed on the ground surface while collecting data for fast investigation along a linear man-made infrastructure such as an airfield. According to Kuras et al. (2006), the DC resistivity measurement is emulated through CCR when the ground resistivity is high such as the dry surface of an embankment. The CCR is therefore a geophysical tool well suited to airfield investigations.

Table 2. Dipole lengths and spacing between the dipoles used for the four runs for each CCR survey line.

Run	Dipole length (m)	Spacing between the dipoles (m)
#1	5	5, 7.5, 10 and 12.5
#2	10	5, 10, 15 and 20
#3	10	25, 30, 35 and 40
#4	10	45, 50, 55 and 60

The apparent electrical resistivities of the airfield embankment and subgrade at Tasiujaq Airport were measured using a Geometrics OhmMapper TR4 system with one transmitter and four receivers operating at a frequency of about 16.5 kHz along three survey lines T-L2, T-L3, and T-L4 over the Southeast side, center line and Northwest side of the airfield embankment respectively (Figure 2). Markers at regular 25-m intervals were put along the survey lines for locating the resistivity measurements relative to the airfield. Four runs with different dipole lengths and spacing between the dipoles were performed for each survey line (Table 2). The variation in spacing between the dipoles changes the depth of investigation for producing pseudo-sections of observed apparent electrical resistivity along the survey lines. The apparent electrical resistivities were then inverted using a quasi-Newton method (Loke and Barker 1996). The models of electrical resistivity found from the inversion of the pseudo-sections are given in Figures 9A and 10 for the three survey lines. The number of iterations for the inversion convergence and the RMS error are given in Figure 10 for each model.

3.2 Ground penetrating radar (GPR) profiles

Ground penetrating radar (GPR) is used for a wide range of subsurface mapping applications to characterize the structure and stratigraphy of near-surface geology. This geophysical tool is made of a pair of transmitting-receiving antennas lying on the ground surface. At each position of the antennas along a survey line, few short electromagnetic impulses at a given nominal frequency are transmitted from the transmitting antenna in the ground and recorded and stacked for amplification by the receiving antenna over a given time period. The radar signal amplitude of each recorded trace is then plotted, one trace against the other, on a travel time profile (Figure 9B). High amplitude on the profile corresponds to a reflection of the radar signal back to the surface from interfaces such as the water table and thawing front characterized by a contrast of dielectric permittivity.

A Sensors & Software pulseEKKO 100 with antennas of 50 MHz was used in the present study to perform two survey types: 1) fixed–offset reflection profile for stratigraphic mapping and 2) common mid–point (CMP) sounding for assessing the velocity of the radar signal in the ground. The GPR profile along the survey line T-L3 is given in Figure 9B. According to the interpretation of two CMP soundings carried out over the field embankment (Figure 2), the radar signal velocity is 0.125 m/ns in the embankment and subgrade. This value was used to transform the GPR travel time profile into a depth profile for assessing the depth of the reflectors (Figure 9B).

3.3 Combined interpretation of CCR and GPR surveys

The combined interpretation of the CCR model of electrical resistivity and GPR profile along the survey line T-L3 over the center line of the airfield embankment takes the form of a cross-section of different stratigraphic units and frozen ground conditions in Figure 9C.

The thickness of the airfield embankment as built (MTQ 1990) is drawn as white and grey dashed lines at a depth of about 2.4 m in Figures 9A and 9B respectively. While a reflector can be associated to the stratigraphic contact between the embankment and the subgrade on the GPR profile (Figure 9B), there is no change in electrical resistivity on the model of electrical resistivity at this contact (Figure 9A). The resistivity of the fluviatile unit which was still frozen on July 2004 (Figure 6) is the same order of the embankment resistivity. The decrease in electrical resistivity at a depth of about 3 m in Figure 9A is due to the contact between the fluviatile unit and the intertidal diamicton. For a salinity of 18 g NaCL/l (Table 1), the freezing point depression is about 1.1 °C and the unfrozen water content of the intertidal diamicton is quite high explaining its low resistivity of 1500 Ω-m in comparison to a value in excess of 10 000 Ω-m for the embankment and fluviatile unit. There is an increase in resistivity at a depth of 7 m from 1500 up to 10 000 Ω-m between 5+430 and 5+800 m associated to the contact between the intertidal diamicton and units of coarse materials (Table 1). At a depth of 13 m, a smooth decrease in resistivity down to 250 Ω-m is induced by the clay unit. The reflectors associated with the contacts between the intertidal diamicton, units of coarse materials, and clay unit are identified with grey full lines on the GPR profile (Figure 9B). The deepest reflector can not be followed all along the survey line (Figure 9B) because the radar signal is too attenuated at the ends of the GPR profile due to the low resistivity values in these sections (Figure 9A). This deepest reflector is also drawn in Figure 9A to show the association between the stratigraphic contact and the decrease in resistivity. The permafrost mound leveled before the airfield construction shows up on a short section of very low resistivity of 100 Ω-m at the Northeast end of the airfield. There is also a section of low resistivity associated with a talik underneath the lake crossed by the airfield between 5+820 and 5+870 m.

The subgrade underneath the two localized zones of thaw subsidence from 5+210 to 5+350 m and from 5+950 to 6+010 m appears in the model of electrical resistivity (Figure 9A) as sections of low resistivity down to 630 Ω-m characteristic of unfrozen conditions in the intertidal diamicton and as deep as 13 m in the units of coarse materials. The subgrade of these sections of the airfield reached a critical thermal state. They are identified as cryotic but unfrozen ground in Figure 9C. The increase in air temperature (Figure 5) and the thermal insulation of snow cover on the Southeast side of the airfield embankment (Figures 7 and 8) induced permafrost warming in the subgrade (Figure 6), increase in unfrozen water content and even melting of the ice lenses in the intertidal diamicton leading to thaw settlement and subsidence of the embankment surface. The subgrade is probably still below 0 °C but unfrozen due to the pore water salinity in the intertidal diamicton depressing its freezing point. The saline pore water in this unit migrated down and contaminated the units of coarse materials also inducing low resistivity in these units.

Most of the airfield embankment lies on the thaw-instable intertidal diamicton and the vulnerability to permafrost degradation of the airfield is considered major.

3.4 Lateral variation in electrical resistivity

The models of electrical resistivity along the three survey lines T-L2, T-L3, and T-L4 over the airfield embankment shown in Figure 10 are for comparison purpose and assessment of lateral variation in electrical resistivity. Only the sections between 5+150 and 5+800 m of the models along the survey lines T-L2, T-L3, and T-L4 are given in Figure 10. The model in Figure 10B is the same as the one in Figure 9A but over the short section. The same resistivity scale is used for all the models.

In addition to the resistive airfield embankment and frozen fluviatile unit more than 10 000 Ω-m over a 3 m thick superficial layer, similar resistivity values for the other units (1500 Ω-m for the intertidal diamicton, near 10 000 Ω-m for the units of coarse materials, and 250 Ω-m for the deep clay unit) are found in all the models for distance larger than 5+350 m (Figure 10). However, the resistivity values of the section between 5+150 and 5+350 are lower and more variable longitudinally and laterally for the three survey lines. As mentioned earlier, the downward migration and contamination of saline pore water from the intertidal diamicton into the units of coarse materials created conduits of low resistivity propagating in the coarse materials. These conduits are clearly visible in the model of electrical resistivity from 5+150 to 5+260 m along the survey line T-L2 (Figure 10A). There is only one such conduit at a distance of 5+230 m in the model of Figure 10B and no conduit at all in the model of Figure 10C. For this last model, even if there is a thinning of the resistivity effect of the units of coarse materials at 11.5 m in depth, the zone of low resistivity due to the intertidal diamicton is still separated from the one of the clay unit all along the survey line T-L4 on the Northwest side of the embankment. Due to the thick snow cover accumulating on the Southeast side (Figures 7 and 8), the permafrost degradation is propagating from the Southeast to the Northwest side. The Southeast side of the embankment is warmer than the Northwest side and the subgrade is therefore less resistive in the Southeast side than the embankment center and Northwest side.

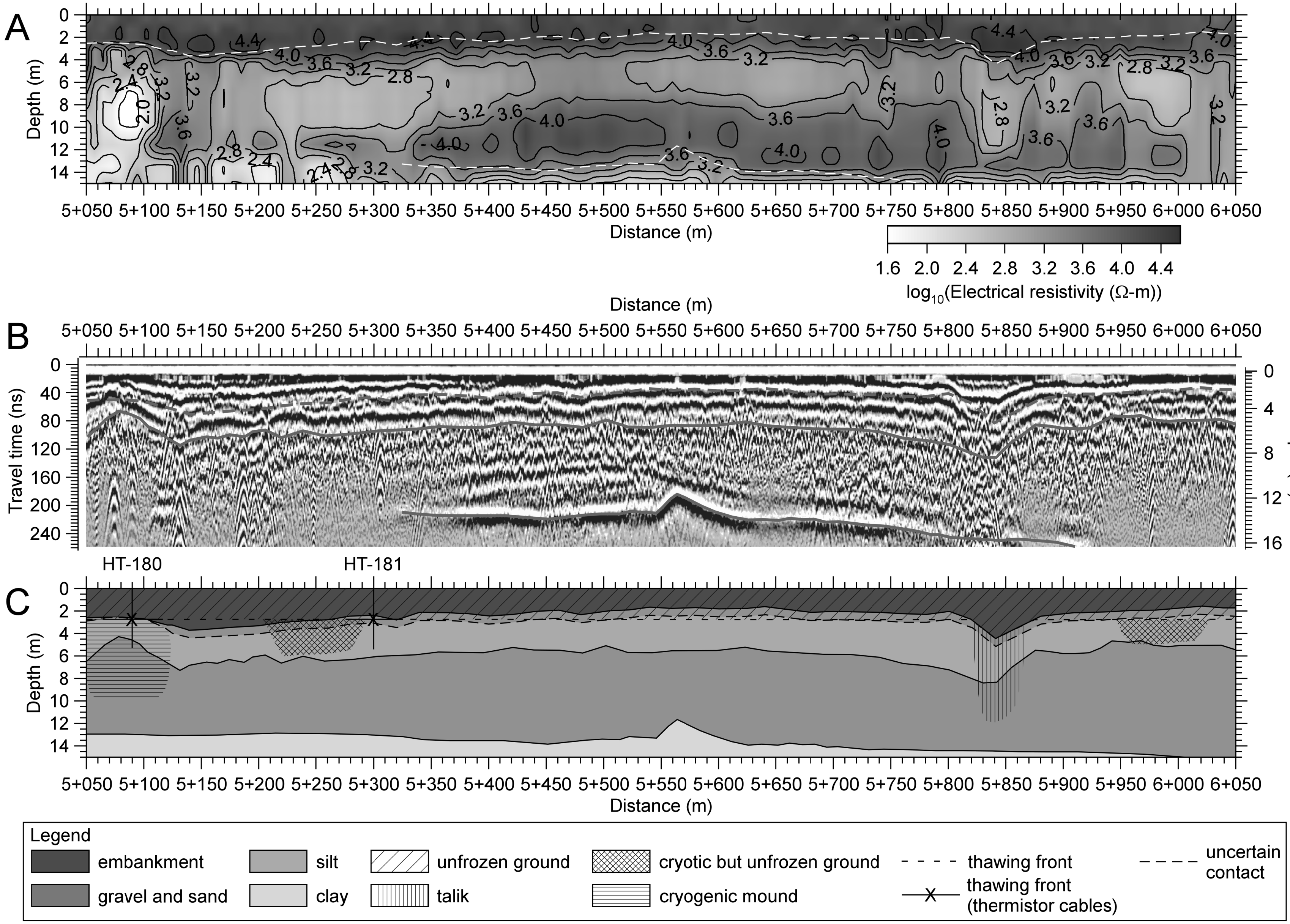

Figure 9. A) Model of electrical resistivity, B) GPR reflection profile, and C) cross-section of the embankment and subgrade along the survey line T-L3 over the center line of the airfield embankment at Tasiujaq Airport, Northern Quebec (Canada). Note the vertical exaggeration (1:10).

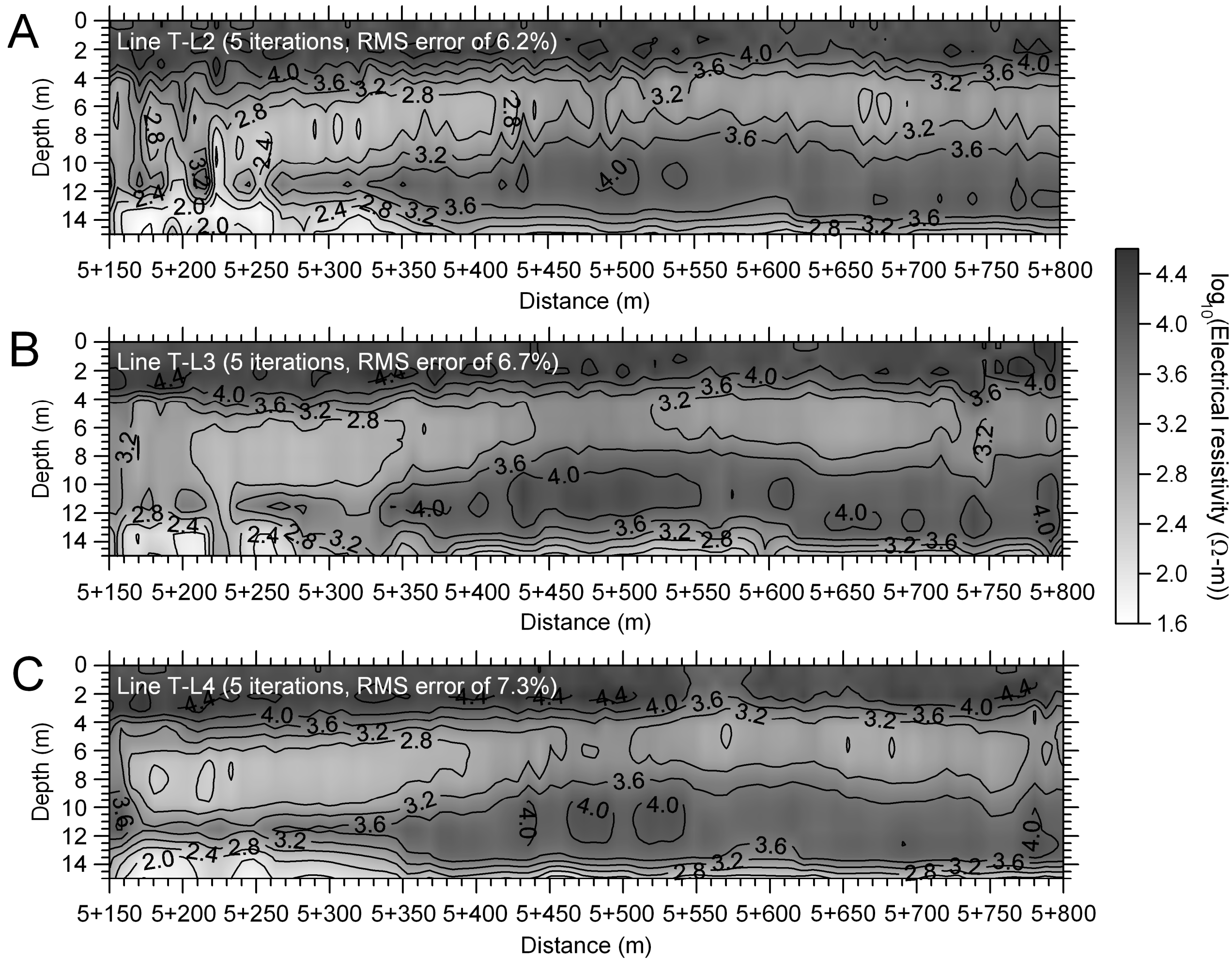

Figure 10. Models of electrical resistivity along the survey lines T-L2 (A), T-L3 (B), and T-L4 (C) over the Southeast side, center line and Northwest side of the airfield embankment respectively at Tasiujaq Airport, Northern Quebec, Canada. See Figure 3 for the location of survey lines T-L2, T-L3, and T-L4. Note the vertical exaggeration (1:10).

CONCLUSIONS

The increase in air temperature in excess of 3 °C over a 10-year period from 1992 to 2002 observed in Northern Quebec (Canada) induced widespread permafrost degradation in the discontinuous permafrost zone mainly under the form of localized zones of thaw subsidence. This permafrost degradation already affects the performance of roads and airfields built on thaw-instable frozen ground. For anticipating and mitigating these impacts, it's critical to assess the frozen ground conditions under these transportation infrastructures and assess their vulnerability to permafrost degradation. Even if the drilling and sampling of permafrost remain the most reliable form of subsurface investigation for ground truth, they are prohibitively expensive in remote areas such as northern communities, they provide only punctual information, and little information is gained on the spatial variability of frozen ground conditions. To overcome these limitations, an engineering geophysical investigation, including capacitively coupled resistivity (CCR) and ground penetrating radar (GPR) surveys, was undertaken in summer 2004 at the airports of Tasiujak, Aupaluk, Kangirsuk and Quaqtaq in Ungava Bay.

The CCR is an effective geophysical tool for characterizing the spatial distribution of frozen ground conditions. However, the model of electrical resistivity found from the inversion of the pseudo-section of apparent electrical resistivity shows smooth contrasts where sharp ones are expected. It does not define well the subsurface stratigraphic contacts. GPR, on the other hand, defines accurately these contacts, but does not provide as much information with respect to the state of permafrost. The combined interpretation of CCR and GPR surveys leads to a high resolution cross-section of frozen ground conditions.

The case study on the Tasiujaq Airport presented herein is a good example of the subsurface characterization capabilities of combined CCR and GPR surveys. According to a stratigraphic cross-section, the airfield embankment lies on a 2.3 m thick layer of intertidal diamicton characterized by ice-poor saline silt and fine sand overlying a 7.9 m thick coarse sand and gravel layer over a deep marine clay layer. The embankment surface is affected by two localized zones of thaw subsidence progressing from the Southeast shoulder to the airfield centre. The permafrost degradation underneath the embankment is taking place in the thaw-instable intertidal diamicton layer. It is due to not only the recent increase in air temperature but also the thermal insulation of snow accumulating on the Southeast shoulder and toe of the airfield embankment. According to the combined interpretation of CCR and GPR surveys, the entire airfield embankment is built on the intertidal diamicton layer overlying the coarse sand and gravel, and clay layers except for the Northeast end where a cryogenic mound was levelled before the airfield construction. The two localized zones of thaw subsidence appear as sections of low electrical resistivity characteristic of unfrozen conditions. The vulnerability to permafrost degradation of the Tasiujaq Airport is major and more thaw subsidence is expected in the future due to the climate warming anticipated over the next decades.

ACKNOWLEDGEMENTS

Funding for this project was provided to Michel Allard, research member of the Centre d'études nordiques, Université Laval, by the Ministère des Transports du Québec, Government of Canada's Climate Change Action Fund, and Ouranos. Thanks are due to D. Fortier, I. Beaulac, F. Vinet, E. L'Hérault, C. Marchildon, D. Saint-Hilaire, and É. Stephani for their help in the field.

REFERENCES

Allard, M. and Seguin, M.-K. 1987. Le pergélisol au Québec nordique : bilan et perspectives, *Géographie physique et Quaternaire*, 61: 141-152.

Calvert, H.T. 2002. Capacitive-coupled resistivity survey of ice-bearing sediments, Mackenzie Delta, *72nd Annual Meeting*, Society of Exploration Geophysicists, Salt Lake City, Utah, USA.

De Pascale, G.P., Pollard, W.H. and Williams, K.K. 2008. Geophysical mapping of ground ice using a combination of capacitive coupled resistivity and ground-penetrating radar, Northwest Territories, Canada, *Journal of Geophysical Research*, 113, F02S90, doi:10.1029/2006JF000585.

Douma, M., Timofeev, V.M., Rogozinski, A.W. and Hunter, J.A. 1994. A capacitive-coupled ground resistivity system for engineering and environmental applications; results of two Canadian field tests, *64th Annual International Meeting*, Society of Exploration Geophysicists, Los Angeles, California, USA, 64: 559-561.

Fortier, R. and Bolduc, M. 2008. Thaw Settlement of Degrading Permafrost: a Geohazard Affecting the Performance of Man-Made Infrastructures at Umiujaq in Nunavik (Québec), *Fourth Canadian Conference on Geohazards*, Québec (QC), Canada, Québec (Québec), Canada: 279-286.

Hauck, C. and Kneisel, C. 2006. Application of capacitively-coupled and DC electrical resistivity imaging for mountain permafrost studies, *Permafrost and Periglacial Processes*, 17: 169-177.

Kuras, O., Beamish, D., Meldrum, P.I. and Ogilvy, R.D. 2006. Fundamentals of the capacitive resistivity technique, *Geophysics*, 71: 135–152.

Loke, M.H. and Barker R. 1996. Rapid least-squares inversion of apparent resistivity pseudo-sections using a quasi-Newton method, *Geophysical Prospecting*, 44: 131-152.

Ministère des Transports du Québec (MTQ) 1990. *Aéroport Tasiujaq V.N. Construction d'une piste, voie de circulation, tablier et route d'accès*, Gouvernement du Québec, CH–85–17–2006, Québec, Canada.

Timofeev, V.M., Rogozinski, A.W., Hunter, J.A. and Douma, M. 1994. A new ground resistivity method for engineering and environmental geophysics, *Proceedings of the Symposium on the Application of Geophysics to Engineering and Environmental Problems*, EEGS: 701-15.